



UNIVERSITY OF LEEDS

This is a repository copy of *Power system stability enhancement through the optimal, passivity-based, placement of SVCs*.

White Rose Research Online URL for this paper:
<http://eprints.whiterose.ac.uk/129148/>

Version: Accepted Version

Proceedings Paper:

Spanias, C, Aristidou, P orcid.org/0000-0003-4429-0225, Michaelides, M et al. (1 more author) (2018) Power system stability enhancement through the optimal, passivity-based, placement of SVCs. In: 2018 Power Systems Computation Conference (PSCC). PSCC 2018, 11-15 Jun 2018, Dublin, Ireland. IEEE . ISBN 978-1-910963-10-4

10.23919/PSCC.2018.8442841

This is an author produced version of a paper which has been accepted to the 20th Power Systems Computation Conference (PSCC 2018).

Reuse

Items deposited in White Rose Research Online are protected by copyright, with all rights reserved unless indicated otherwise. They may be downloaded and/or printed for private study, or other acts as permitted by national copyright laws. The publisher or other rights holders may allow further reproduction and re-use of the full text version. This is indicated by the licence information on the White Rose Research Online record for the item.

Takedown

If you consider content in White Rose Research Online to be in breach of UK law, please notify us by emailing eprints@whiterose.ac.uk including the URL of the record and the reason for the withdrawal request.



eprints@whiterose.ac.uk
<https://eprints.whiterose.ac.uk/>

Power system stability enhancement through the optimal, passivity-based, placement of SVCs

Chrysovalantis Spanias*, Petros Aristidou†, Michalis Michaelides*, Ioannis Lestas‡

* Department of Electrical Engineering, Computer Engineering and Informatics, Cyprus University of Technology, Cyprus

† School of Electronic and Electrical Engineering, University of Leeds, Leeds LS2 9JT, UK

‡ Department of Engineering, University of Cambridge, Trumpington Street, Cambridge CB21PZ, UK

Emails: ca.spanias@edu.cut.ac.cy, p.aristidou@leeds.ac.uk, michalis.michaelides@cut.ac.cy, icl20@cam.ac.uk

Abstract—Over the last decades, several techniques have been proposed for the optimal placement of FACTS devices across power systems. Although these techniques were shown to improve power system operation, they are usually computationally intractable while having serious inherent limitations. In this paper, we present a novel approach to guide the SVC location identification in order to enhance power system stability. Specifically, the proposed method exploits findings in passivity-based control analysis and design in order to address the most vulnerable -in terms of passivity- buses of the system and consequently the optimal locations for SVC installation. We then show how the incorporation of SVCs at the aforementioned buses can passivate the system and provide guarantees for increased stability. Furthermore, we provide a brief discussion regarding the sizing and the number of required SVC devices in order to guarantee such stability improvement. Finally, we illustrate our results with simulations on the IEEE 68 bus system and show that both the dynamic response and the damping of the system are significantly improved.

Index Terms—power system stability enhancement, passivity, Static Var Compensator (SVC), optimal placement

I. INTRODUCTION

During the last decade, there has been a constant societal push to make electric power systems more sustainable and economical. This push along with the new increased electricity demands has resulted in current power systems operating close to their stability and loadability limits. Flexible AC Transmission System (FACTS) devices have been identified as ideal to improve system stability and increase these limits [1]. However, due to their high cost, their location in the network should be carefully selected to maximize the stabilizing effects.

Several techniques based on either optimization procedures or sensitivity and stability indices have been proposed in the past [2]–[7]. Optimization techniques require tackling non-linear, mixed integer, problems which can prove computationally intractable. At the same time, techniques based on indices coming from the linearization of the system have inherent limitations [8].

Recent studies have shown that the principle of passivity can be used to assess the stability of large-scale systems and to design appropriate controls that can enhance system performance [9]–[12]. An interesting feature of this key structural property is the ability to perform the analysis locally and

combine the results to decide about the stability of the entire system. This allows identifying the “weaker” areas of the system through the lack of passivity and selecting the optimal location of FACTS devices to passivate the entire system and provide guarantees for stability and robustness.

In this paper, we propose a novel, optimal placement technique for Static Var Compensator (SVC) devices to enhance system stability. This method exploits findings in passivity-based control analysis and design to guide the SVC location installation. It should be mentioned that the methodology proposed in the next sections can be easily applied to the placement of other types of FACTS devices. However, for simplicity, in this work, we will only deal with the placement of SVCs.

First, we describe the dynamic models used to represent the power system components within the proposed approach. The models use the multi-variable, system reference-frame approach presented in [12]. Then, by considering that every power network with arbitrary topology satisfies certain passivity properties [12], we identify the passivity indices revealed when the loads are incorporated into the analysis. These passivity indices are derived through the formation of an aggregate network model that describes the power grid while capturing the effect of the loads as well. The proposed placement approach is then formulated by identifying the areas in the aggregate model where the passivity condition is violated. Particularly, we identify the most vulnerable -in terms of passivity- buses of the system and consequently the optimal locations for the SVC installation. SVCs are then applied to these locations in order to “passivate” the aggregate network model via feed-forward passivation [13]. We, therefore, achieve to guarantee the overall enhancement of the power system stability while providing important information regarding the sizing and the number of required SVC devices.

Our findings are illustrated through dynamic simulations on the IEEE 68-bus test system, where we use the developed technique to drive the SVC installation considering an average loading of the system. A significantly improved response of the system is achieved during a generation-load imbalance, even when only a small percentage of buses is equipped with SVCs. The effectiveness of the proposed passivity-base approach for the SVC placement is also supported by monitoring the power system oscillatory modes.

The rest of the paper is organized as follows: In Section II, we present the models for the network, the SVC and the loads. The passivity properties satisfied within the power systems are provided in Section III. Section IV then presents the passivity-based approach for the optimal placement of SVCs, while also providing a brief discussion regarding the sizing and the number of the required SVC devices. In Section V, we illustrate our results through simulations on the IEEE 68 bus system. Finally, conclusions are drawn in Section VI.

II. PRELIMINARIES

In this section, we describe the models that are used to represent the power network, the SVCs and the loads. All models are formulated as multi-input/multi-output systems and expressed in the system reference-frame i.e., two common axes rotating at synchronous frequency ω_s .

A. Power network model

A power network with arbitrary topology can be described by a connected and undirected graph $(\mathcal{N}, \mathcal{E})$, where $\mathcal{N} = \{1, 2, \dots, |\mathcal{N}|\}$ is the set of buses and $\mathcal{E} \subset \mathcal{N} \times \mathcal{N}$ the set of transmission lines connecting them. We use (i, j) to denote the link connecting the network buses i and j .

For the derivation of the equations describing the network, we consider the following assumptions.

Assumption 1: Transmission lines are represented by symmetric three-phase RLC elements and modeled by their Π -equivalent.

Assumption 2: Transmission line dynamics evolve on a much faster timescale than the dynamics of the generation sources and the loads.

According to Assumption 2, the transmission lines reach steady state much earlier than the generators and the loads. The power network can therefore be modeled by the network current flows given by the nodal set of equations:

$$\bar{I} = Y^N \bar{V} \quad (1)$$

where Y^N is the $\mathbb{C}^{|\mathcal{N}| \times |\mathcal{N}|}$ bus admittance matrix of the network. $\bar{I} \in \mathbb{C}^{|\mathcal{N}|}$ and $\bar{V} \in \mathbb{C}^{|\mathcal{N}|}$ denote the net injected current and the bus voltage vectors respectively. The elements of the net injected current and the bus voltage vectors are both expressed in phasor form since the analysis assumes balanced and symmetric operating conditions.

The nodal admittance matrix Y^N is a complex symmetric matrix which can be written in rectangular form as

$$Y^N = G^N + jB^N \quad (2)$$

where $G^N, B^N \in \mathbb{R}^{|\mathcal{N}| \times |\mathcal{N}|}$ are the network's conductance and the susceptance matrices respectively. G^N and B^N are both real, $|\mathcal{N}| \times |\mathcal{N}|$, sparse symmetric matrices.

Similarly to the nodal admittance matrix, the net injected current and bus voltage vectors are also expressed in the rectangular complex form to develop the analytic network

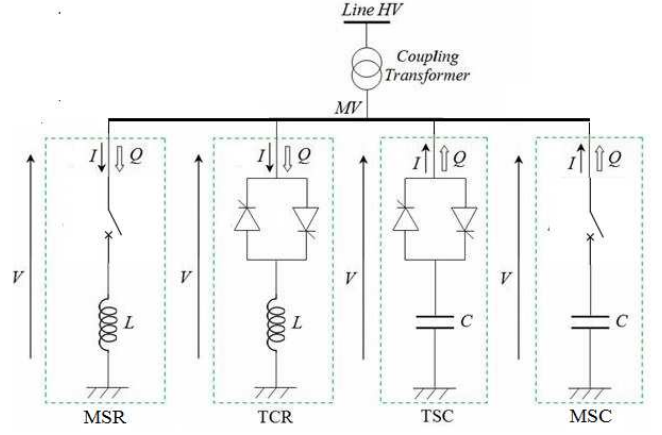


Figure 1. Example of SVC structure

equations. The net injected currents and bus voltages can therefore be written as

$$\bar{I}_i = I_i \angle \phi_{I,i} = I_i \cos \phi_{I,i} + j I_i \sin \phi_{I,i} = I_{a,i} + j I_{b,i} \quad (3)$$

$$\bar{V}_i = V_i \angle \phi_{V,i} = V_i \cos \phi_{V,i} + j V_i \sin \phi_{V,i} = V_{a,i} + j V_{b,i} \quad (4)$$

for all $i \in \mathcal{N}$. We now define the vectors $I_a = [I_{a,1} \ I_{a,2} \ \dots \ I_{a,|\mathcal{N}|}]^T$, $I_b = [I_{b,1} \ I_{b,2} \ \dots \ I_{b,|\mathcal{N}|}]^T$, $V_a = [V_{a,1} \ V_{a,2} \ \dots \ V_{a,|\mathcal{N}|}]^T$ and $V_b = [V_{b,1} \ V_{b,2} \ \dots \ V_{b,|\mathcal{N}|}]^T \in \mathbb{R}^{|\mathcal{N}|}$, and the net injected current and the bus voltage vectors are thus given in the following form:

$$\bar{I} = I_a + j I_b \quad (5)$$

$$\bar{V} = V_a + j V_b \quad (6)$$

respectively. By substituting equations (2) and (5)-(6) into (1) we get:

$$\bar{I} = I_a + j I_b = (G^N V_a - B^N V_b) + j (B^N V_a + G^N V_b) \quad (7)$$

where

$$I_a = G^N V_a - B^N V_b \quad (8)$$

$$I_b = B^N V_a + G^N V_b. \quad (9)$$

From (8), (9) we deduce the net injected current components, $I_{a,i}$ and $I_{b,i}$, at each bus $i = 1, 2, \dots, |\mathcal{N}|$, which are given by:

$$I_{a,i} = \sum_{j=1}^{|\mathcal{N}|} (G_{ij}^N V_{a,j} - B_{ij}^N V_{b,j}) \quad (10)$$

$$I_{b,i} = \sum_{j=1}^{|\mathcal{N}|} (B_{ij}^N V_{a,j} + G_{ij}^N V_{b,j}) \quad (11)$$

Finally, we derive the power network model as a $(2 \times |\mathcal{N}|)$ -input/ $(2 \times |\mathcal{N}|)$ -output system, similarly to [12], and we write (8)-(9) in a compact matrix form as follows:

$$\underbrace{\begin{bmatrix} I_a \\ I_b \end{bmatrix}}_{y^n} = \underbrace{\begin{bmatrix} G^N & -B^N \\ B^N & G^N \end{bmatrix}}_{H^N} \begin{bmatrix} V_a \\ V_b \end{bmatrix} \quad (12)$$

B. SVC model

Typically, a SVC comprises of one or more banks of fixed or switched shunt capacitors or reactors, of which at least one bank is switched by thyristors. A typical structure of a SVC installation is illustrated in Fig. 1.

Although several detailed models have been proposed in the literature to capture the dynamic characteristics of SVCs, in this paper, we derive a simple, linearized model which facilitates our analysis but still captures the necessary dynamics. The model is based on the *Basic Model 1* presented in [14] and is described by

$$B_i^{\text{svc}}(s) = \frac{K_R \cdot (1 + sT_1)}{(1 + sT_R)(1 + sT_2)} \quad (13)$$

where the variables B_i^{svc} , V_i^{ref} and V_i denote the SVC susceptance, the reference voltage, and the voltage magnitude at bus i , respectively. K_R is the regulator gain constant while T_R , T_1 and T_2 are the regulator and compensator lead and lag time constants, respectively. The aforementioned model is widely used in several dynamic simulation programs such as PST [15], even though it omits the SVC measurement and the thyristor susceptance control modules. The model (13), has a susceptance range which can be easily computed by the formulas given in [14].

In order to derive a $(2 \times |\mathcal{N}|)$ -input/ $(2 \times |\mathcal{N}|)$ -output system similarly to the network model (12), we transform the transfer function (13) into state-space form. Next, by considering that the mappings of the current output of the SVC are given by

$$\bar{I}_i = jB_i^{\text{svc}}\bar{V}_i \rightarrow I_{a,i} = -B_i^{\text{svc}}V_{b,i} \text{ and } I_{b,i} = B_i^{\text{svc}}V_{a,i}$$

and that $V_i = \sqrt{V_{a,i}^2 + V_{b,i}^2}$ and $I_i = \sqrt{I_{a,i}^2 + I_{b,i}^2}$ we get the following multi-variable system

$$\begin{bmatrix} I_{a,i} \\ I_{b,i} \end{bmatrix} = \underbrace{\begin{bmatrix} T_i^a(s) & T_i^b(s) + B_i^{\text{svc}} \\ -T_i^b(s) - B_i^{\text{svc}} & T_i^a(s) \end{bmatrix}}_{H_i^{\text{svc}}(s)} \begin{bmatrix} V_{a,i} \\ V_{b,i} \end{bmatrix}. \quad (14)$$

We note here that the above system is derived through the linearization of the SVC model (13) around its operating point. $H_i^{\text{svc}}(s)$ denotes the 2×2 proper transfer function matrix relating the voltage components $V_{a,i}$ and $V_{b,i}$ with the current components $I_{a,i}$ and $I_{b,i}$ while the transfer functions $T_i^x(s)$ are given by

$$T_i^x(s) = \frac{K_i^x \cdot (1 + sT_1)}{(1 + sT_R)(1 + sT_2)}. \quad (15)$$

where $x \in \{a, b\}$. The gain constants K_i^x (i.e., K_i^a and K_i^b) are derived through the linearization procedure and satisfy the following inequalities

$$K_i^a \geq K_i^b \geq 0. \quad (16)$$

Remark 1: The multi-variable model (14) that we adopt in this paper, captures both the capacitive and the inductive operation of SVCs.

C. Load model

Loads are represented by a dynamic model modified from [16] so as to fit our multi-variable framework. Considering that for every load the following hold

$$\bar{I}_i = I_{a,i} + jI_{b,i} = -(G_i^L - B_i^L)V_{a,i} - j(G_i^L + B_i^L)V_{b,i} \quad i \in \mathcal{N}$$

the load model is given by

$$\begin{bmatrix} I_{a,i} \\ I_{b,i} \end{bmatrix} = \underbrace{\begin{bmatrix} -G_i^L(s) & B_i^L(s) \\ -B_i^L(s) & -G_i^L(s) \end{bmatrix}}_{H_i^L(s)} \begin{bmatrix} V_{a,i} \\ V_{b,i} \end{bmatrix} \quad (17)$$

where $H_i^L(s)$ denotes the 2×2 transfer function matrix that describes the dynamic behavior of loads. The matrices $G_i^L(s)$ and $B_i^L(s)$ present the dynamic behavior of the resistive and inductive/capacitive parts of the loads, respectively.

In the case of a constant impedance load, the model of (17) can be further simplified as:

$$\begin{bmatrix} I_{a,i} \\ I_{b,i} \end{bmatrix} = \underbrace{\begin{bmatrix} -G_i^L & B_i^L \\ -B_i^L & -G_i^L \end{bmatrix}}_{H_i^L} \begin{bmatrix} V_{a,i} \\ V_{b,i} \end{bmatrix} \quad (18)$$

where $H_i^L \in \mathbf{R}^{2 \times 2}$ is now the matrix relating the voltage components with the net injected current components in the same manner as H^N in the network model formulation. G_i^L and B_i^L are constant, time-invariant values. The negative sign in the aforementioned models appears due to the fact that $I_{a,i}$ and $I_{b,i}$ denote the components of the net absorbed current rather than the net injected current.

III. PASSIVITY INDICES WITHIN POWER NETWORKS

A. Passivity of the network model

In order to examine the passivity property that is revealed for the network system through the aforementioned multi-variable modeling, we first provide the following fundamental passivity definition [17].

Definition 1: Consider the system described by the memoryless function $y = g(t, u)$ where $g : [0, \infty) \times \mathbb{R}^p \rightarrow \mathbb{R}^p$. This system is passive if $u^T y \geq 0$.

As stated above, the static network model (12) is passive only when the inequality of Definition 1 is satisfied, that is

$$u^T y = [V_a^T \ V_b^T] \begin{bmatrix} I_a \\ I_b \end{bmatrix} \geq 0 \quad (19)$$

for all $V_a, V_b, I_a, I_b \in \mathbb{R}^{|\mathcal{N}|}$.

Lemma 1: The network system defined in (12) with inputs the vectors of bus voltage components $[V_a^T \ V_b^T]^T$ and outputs the vectors of net injected current components $[I_a^T \ I_b^T]^T$ is passive.

Proof of Lemma 1: By substituting the network equations (12) in inequality (19) we get

$$\begin{aligned} u^T y &= [V_a^T \ V_b^T] H^N \begin{bmatrix} V_a \\ V_b \end{bmatrix} = [V_a^T \ V_b^T] \begin{bmatrix} G^N & -B^N \\ B^N & G^N \end{bmatrix} \begin{bmatrix} V_a \\ V_b \end{bmatrix} \\ &= V_a^T G^N V_a + V_b^T G^N V_b \geq 0 \end{aligned} \quad (20)$$

for all $V_a, V_b \in \mathbb{R}^{|\mathcal{N}|}$. The inequality (20) reveals that the passivity of the network is ensured when the composite matrix H^N , or equivalently its diagonal elements G^N , are positive semidefinite matrices.

$G^N \in \mathbb{R}^{|\mathcal{N}| \times |\mathcal{N}|}$ is a square, sparse, symmetric, matrix with non-negative diagonal and negative off-diagonal elements, i.e., $G_{ii}^N \geq 0$ and $G_{ij}^N \leq 0 \forall i, j = 1, 2, \dots, |\mathcal{N}|$. It is also diagonally dominant as the following equation holds:

$$|G_{ii}^N| = \sum_{j \neq i}^{|\mathcal{N}|} |G_{ij}^N| \Leftrightarrow G_{ii}^N = - \sum_{j \neq i}^{|\mathcal{N}|} G_{ij}^N, \quad (i, j) \in \mathcal{E} \quad (21)$$

In order to prove the positive semidefiniteness of the matrix G^N , we make use of the Geshgorin Circle Theorem [18]. We therefore define the Geshgorin discs $D_i(G_{ii}^N, R_i)$, $i = 1, 2, \dots, |\mathcal{N}|$ of the matrix G^N . D_i is a closed disc centered at $(G_{ii}^N, 0)$, with radius $R_i = \sum_{i \neq j} |G_{ij}^N|$. As stated above the matrix G^N has positive diagonal elements and is also diagonally dominant. Subsequently, its Geshgorin discs lie in the right half plane, have center on the real axis and are tangent to the imaginary axis since $G_{ii}^N - R_i = 0, \forall i = 1, 2, \dots, |\mathcal{N}|$. According to the Geshgorin circle theorem, the eigenvalues of the matrix G^N lie within its Geshgorin discs, corresponding to its columns (or equivalently to its rows). Subsequently, G^N has eigenvalues with non negative real parts which immediately leads to the fact that it is positive semidefinite [19]. Condition (19) is therefore satisfied. \square

We see within the proof of Lemma 1 that the condition (19) always holds and the passivity of the system's network is ensured regardless of its topology. Specifically, due to the form of the composite matrix H^N , the positive semidefiniteness of the network's conductance matrix G^N is sufficient for the condition (19) to be satisfied. G^N in turn, is always positive semidefinite since it has positive diagonal elements and its diagonal dominance is never violated.

B. Load effect

We are now about to examine how the grid connected loads affect the passivity of the network model (12). In the previous section, we considered that each load bus forms a 2-input/2-output system while any bus that does not consist of any load is represented by zero dynamics. Thus, we define the following aggregate model which is derived by the parallel interconnection of the network and the aggregate load dynamics. The combined model is given by

$$\begin{aligned} \begin{bmatrix} I_a \\ I_b \end{bmatrix} &= H^{AGG} \begin{bmatrix} V_a \\ V_b \end{bmatrix} = (H^N + H^L) \begin{bmatrix} V_a \\ V_b \end{bmatrix} \\ &= \begin{bmatrix} G^N - G^L & -B^N + B^L \\ B^N - B^L & G^N - G^L \end{bmatrix} \begin{bmatrix} V_a \\ V_b \end{bmatrix} \end{aligned} \quad (22)$$

where H^{AGG} and H^L denote the transfer function matrices of the aggregate network model and all the grid connected loads respectively. The aggregate model (22) can be further simplified under the consideration of constant impedance loads (18).

As we observe from both the load models (17)-(18), loads constitute a non-passive system since the matrices $H_i^L(s)$ and H_i^L do not satisfy the requirement of positive realness and positive semidefiniteness respectively [20]. Thus, the incorporation of the loads into the network model (aggregate model (22)) results in the violation of its passivity. Equivalently, due to the fact that the aggregate model (22) is derived by the parallel interconnection of the network and the load systems, we can also say that it has a shortage of passivity or it lacks Input Feed-forward Passivity (IFP) [13].

Remark 2: In the current section, we provided a brief overview of the passivity indices within power systems. However, we did not discuss how the generators, which are the most vital components of a power grid, affect its overall passivity. As discussed in [9], [21], [22], synchronous generators usually constitute passive dynamical systems which can guarantee the asymptotic stability of the power system, or can be passivated with sufficiently high damping. This is also verified in [12] with examples involving more advanced generator models formulated at the system reference frame.

IV. OPTIMAL PLACEMENT OF SVCs

In this section, we investigate the optimal SVC placement for enhancing the overall stability of the power system. First, we assess each bus vulnerability index – in terms of passivity – and then explain how SVCs can passivate the aggregate network model and subsequently enhance the power system stability. Finally, a brief discussion regarding the sizing and the number of the required SVC devices in order to guarantee the power system stability enhancement is also provided.

A. Bus vulnerability assessment

In order to address the network's vulnerable buses, we follow a novel, yet effective, approach based on the Geshgorin Circle Theorem which was employed for the proof of the passivity of the network model (Lemma 1). We should note here that in order to facilitate our analysis for the identification of the vulnerable buses of the grid we adopt the constant impedance load model (18).

As mentioned in Section III, the passivity of the network model is guaranteed due to the diagonal dominance of the conductance matrix of the network G^N . However, the incorporation of the grid connected loads into our analysis results in the violation of the network's passivity which is now represented by (22). The passivity of the aggregate network model (22) depends now on the positive definiteness of the aggregate conductance matrix $G^{AGG} = G^N - G^L$. Due to the fact that the load conductance matrix $-G^L$ constitutes a diagonal matrix with non-positive diagonal elements, the Geshgorin discs corresponding to the respective columns/rows of G^{AGG} are now displaced by G_{ii}^L towards the left half plane, thus violating the passivity property of the power network. The graphical illustration of the effect of the load incorporation into the power network analysis is presented in Fig. 2.

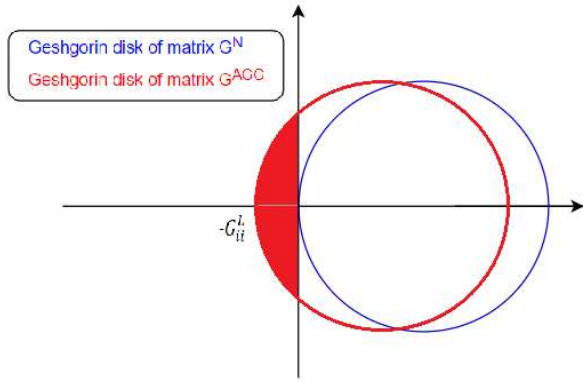


Figure 2. Graphical representation of the Geshgorin disks corresponding to the i^{th} column/row (bus i) of the matrices G^N and G^{AGG} .

We therefore define the Geshgorin discs $D_i'(G_{ii}^{AGG}, R_i')$ of the aggregate conductance matrix where the diagonal element G_{ii}^{AGG} defines the center and R_i' the radius of the disc corresponding to the column/row $i = 1, 2, \dots, |\mathcal{N}|$. Each bus $i \in \mathcal{N}$ vulnerability index can now be calculated as the percentage of the Geshgorin disk that lies in the left half plane. The vulnerability index of bus i is therefore given by

$$v_i = A_i' / A_i \times 100 \quad (23)$$

where A_i' and A_i denote the area of the disk lying at the left half plane and the total area of the Geshgorin disc i respectively. A large vulnerability index indicates a large probability for H^{AGG} to have an eigenvalue in the left half plane. This could increase the possibility for the power system to exhibit an oscillatory behavior due to the violation of the passivity property.

B. Feed-forward passivation of the power network

Passivation is the procedure to render a system that lacks passivity passive via either feed-back or feed-forward interconnection [13]. Due to the fact that passive systems are stable and easy to control, passivation is often a useful tool in control design. In this paper, we identify the optimal locations for SVC installation in order to achieve the feed-forward passivation of the power network and thus to improve power system stability. Before presenting how the power network is passivated through the SVC installation we first provide the following passivity definition regarding Linear Time Invariant (LTI) systems.

Definition 2: Let a dynamic system represented in Laplace domain by its $p \times p$ proper rational transfer function matrix $G(s)$. The aforementioned system is passive if $G(s)$ is positive real, i.e.

- poles of all elements of $G(s)$ are in $Re(s) \leq 0$
- for all real ω for which $j\omega$ is not a pole of any element of $G(s)$, the matrix $G(j\omega) + G^T(-j\omega)$ is positive semidefinite, and
- any pure imaginary pole $j\omega$ of any element of $G(s)$ is a simple pole and the residue matrix $\lim_{s \rightarrow j\omega} (s - j\omega)G(s)$ is positive semidefinite Hermitian.

Lemma 2: If the time constants of the SVC are selected such that $T_2 \cdot T_R / (T_2 + T_R) \leq T_1 \leq 1 + T_2 + T_R$, the SVC model defined in (14) is passive.

Proof of Lemma 2: Since all time constants of the SVC model (14) are real and positive, it is straightforward to prove the first and the third conditions in Definition 2, that is, the poles of all elements of $H_i^{\text{svc}}(s)$ are real and lie in the left half plane.

From the SVC model (14), we now compute the sum of the SVC transfer function matrix and its conjugate transpose, i.e.

$$\begin{aligned} H_i^{\text{svc}}(j\omega) + H_i^{\text{svc}}(-j\omega)^T &= \\ &= \frac{2}{(1 + \omega^2 T_2^2)(1 + \omega^2 T_2^2)} \begin{bmatrix} K_i^a \hat{K} & jK_i^b \bar{K} \\ -jK_i^b \bar{K} & K_i^a \hat{K} \end{bmatrix} \end{aligned} \quad (24)$$

where $\hat{K} = 1 + \omega^2(T_1(T_2 + T_R) - T_2 T_R)$ and $\bar{K} = T_1 - T_2 - T_R - \omega^2 T_1 T_2 T_R$. Considering that $\hat{K} \geq 0$, time constants T_1 , T_2 and T_R are selected as stated within the Lemma 2, and condition (16) holds,

$$H_i^{\text{svc}}(j\omega) + H_i^{\text{svc}}(-j\omega)^T \geq 0 \quad (25)$$

for all ω . The second condition of Definition 2 is therefore satisfied, and the SVCs constitute passive systems. \square

We therefore consider that SVCs are applied to the optimal locations across the grid. The aggregate network model (22) now becomes:

$$\begin{bmatrix} I_a \\ I_b \end{bmatrix} = H^{AGG'} \begin{bmatrix} V_a \\ V_b \end{bmatrix} = (H^N + H^L + H^{\text{svc}}) \begin{bmatrix} V_a \\ V_b \end{bmatrix} \quad (26)$$

where $H^{AGG'}$ and H^{svc} denote the transfer function matrices of the modified aggregate network and all grid connected SVCs respectively. The feed-forward passivation of the aggregate network model (22) is now carried out via the parallel interconnection of passive systems at the most vulnerable - in terms of passivity - buses of the grid. Consequently, this results to the power system stability enhancement and also the reduction of the reactive power flows across the power grid.

Remark 3: We should note that the proposed approach can be further exploited in order to incorporate other FACTS devices, such as TCSCs, UPFCs etc. These devices not only could improve the power system stability, but they could also increase the transmission system transfer capability and further reduce the transmission losses [1].

Remark 4: An effective method to verify if whole power system is passive, it is the use of the Kalman-Yakupovich-Popov (KYP) lemma [17]. Particularly, KYP lemma can be employed within a Linear Matrix Inequality (LMI) problem in order to verify the passivity of the whole system as extensively described in [23, Section 2].

C. Location and Sizing of SVCs

The proposed technique allows identifying the buses that violate passivity. These can be sorted according to their severity based on the vulnerability index v_i . In order to then passivate the system, an SVC can be connected to each of the violating buses to counteract the effect of the load. The size of each individual SVC can be computed through the value of K_i

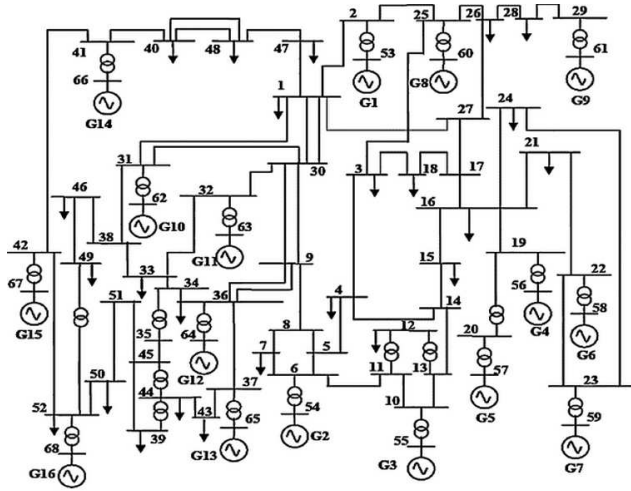


Figure 3. Single line diagram of the IEEE 68-bus test system (New York / New England).

(see Eq. 15) necessary to shift the Geshgorin disk to the right-hand side while its time constants shall fulfill the requirements stated in Lemma 2. This can be seen visually in Fig. 2. The passivity of the entire system can then be verified by applying the KYP lemma (see Remark 3) on the new system including the SVCs.

However, due to the local effect of each SVCs, in order to passivate the entire system, we would need as many SVCs as the number of violated buses. The actual number of SVCs required will be smaller as the synchronous generators will provide some passivation to the system and can then be derived by employing the KYP lemma described in the previous subsection (see Remark 4).

While passivating the entire system would provide some certificates for the system stability, it is usually not cost effective. Moreover, passivity provides more conservative boundaries for the system. Alternatively to passivating the entire system, when only a specific SVC “budget” is available (in terms of size and number of SVCs), then the previous procedure can be used to prioritize the installation based on the vulnerability index.

V. SIMULATION RESULTS

In this section we verify our framework using the IEEE New York / New England 68-bus interconnection system [24], which is presented in Fig. 3. The aforementioned testbed system consists of 16 generator and 24 load buses. The generators and the loads are represented by the fourth-order synchronous generator model and the ZIP model respectively [25]. The generators are equipped with turbine governors, a simple excitation system and Power System Stabilizers (PSSs) while loads include induction motors as well.

Considering a “budget” of 14 SVCs, we prioritize their installation in order to achieve the greatest stability improvement possible. We thus compute the vulnerability indices of the network using the method proposed within the current paper and find the most vulnerable buses of the testbed system, i.e.

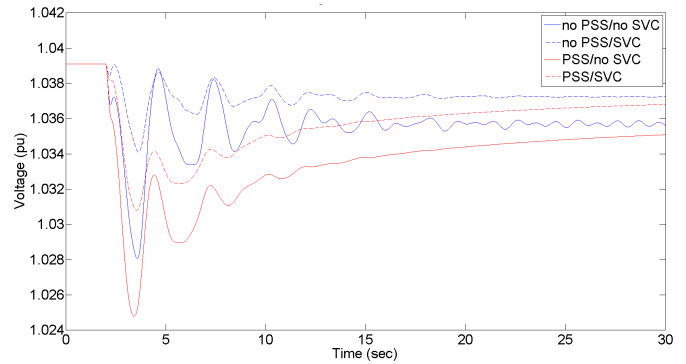


Figure 4. The voltage deviation at bus 9.

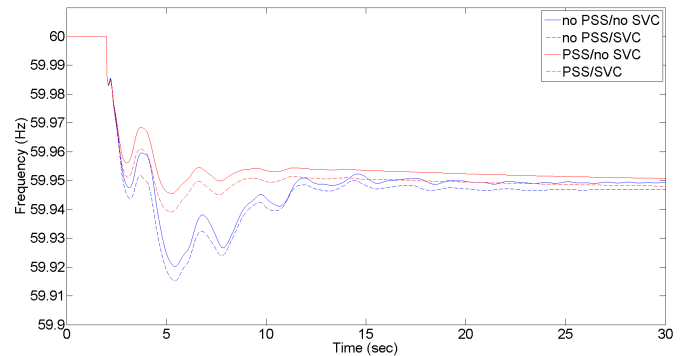


Figure 5. The frequency deviation at bus 9.

3, 4, 8, 15, 21, 23, 24, 28, 45, 46, 48, 49, 50, 51. The provided SVCs have the following prefixed characteristics: $K_R = 20$ pu, $T_R = 0.05$ s, $T_1 = 0.65$ s and $T_2 = 0.2$ s.

Our approach is verified through a dynamic simulation and an eigenanalysis of the test system, using the Power System Toolbox (PST) [15]. Both the dynamic simulation and the eigenanalysis are carried out considering average loading, for the following four different cases: (i) no PSSs applied on generators / no SVCs installed at the grid, (ii) no PSSs applied on generators / SVCs installed at the grid, (iii) PSSs applied on generators / no SVCs installed at the grid, and (iv) PSSs applied on generators / SVCs installed at the grid.

For the dynamic simulation, we apply a step load change of 100 MW to the load buses 1, 7, 21 and 40. The enhancement of the system’s stability is illustrated by the voltage and the frequency deviation at bus 9, shown in Figs. 4 and 5, respectively. As observed, the proposed SVC placement results in a significantly improved response and the suppression of the occurring oscillations either when PSSs are applied to the excitation systems of the generators or not.

The stability enhancement achieved through the proposed approach is also illustrated through the eigenanalysis of the test system. As it can be seen from Fig. 6, the application of SVCs using the proposed technique damps the calculated modes when PSSs are either applied to the generators or not. More specifically, for the case (i) the system is small-signal unstable since there exists an eigenvalue on the positive real

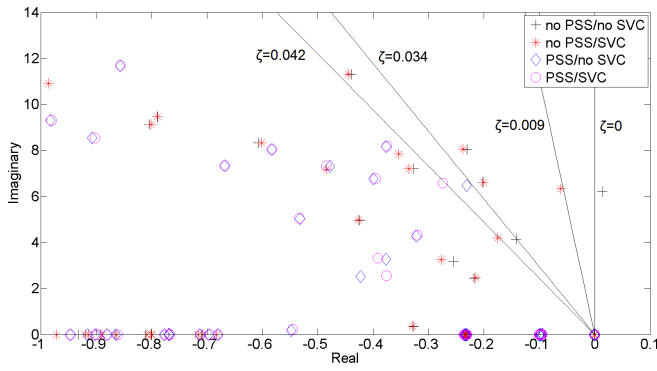


Figure 6. Eigenanalysis of the IEEE 68 bus test system.

axis. The application of SVCs on the most vulnerable buses (case (ii)) stabilizes the system moving all the eigenvalues to the left half plane. Moreover, all the modes have a better damping ratio¹ when the SVCs are connected. Although the application of PSSs on the excitation systems of the generators improves further the small-signal stability of the test system, the SVC installation at the selected locations results in a more stable response. The damping ratio of both the local and the interarea modes of the system is significantly increased for the cases (iii) and (iv), respectively.

Finally, it should be noted here that the SVCs were not designed to provide oscillation damping or target any specific oscillatory modes. The stability improvement arises through the passivation of the system. While not considered in this paper, the application of a Power Oscillation Damping controller to the installed SVCs could facilitate the damping of inter-area oscillations and further enhance system stability. In particular, by measuring the local frequency at the SVC bus, we can design an SVC control to also target specific system modes, similarly to the PSS.

VI. CONCLUSIONS

In this paper, we proposed a novel passivity-based technique for the optimal placement of SVCs to improve the power system stability and robustness. We first introduced the models describing the network, the SVCs and the loads, which were formulated as multi-input/multi-output systems. We then provided the passivity indices arising within the power system under such formulation and proposed a novel way to identify the grid's optimal locations and sizing for SVC installation. Based on the local load size and behavior, we employed the feature of the feed-forward passivation in order to passivate the power system and thus enhance its stability. Finally, we illustrated the effectiveness of the presented technique on the IEEE 68 bus test system by applying SVCs to the fourteen most vulnerable buses of the system.

REFERENCES

[1] N. G. Hingorani and L. Gyugyi, *Understanding facts*. IEEE press, 2000.

¹The damping ratio of an eigenvalue $\lambda = a + j\beta$ is defined as $\zeta = -\frac{a}{\sqrt{a^2 + \beta^2}}$.

- [2] E. Ghahremani and I. Kamwa, "Optimal placement of multiple-type facts devices to maximize power system loadability using a generic graphical user interface," *IEEE Transactions on Power Systems*, vol. 28, pp. 764–778, May 2013.
- [3] R. Miguez, F. Milano, R. Zrate-Miano, and A. J. Conejo, "Optimal network placement of svc devices," *IEEE Transactions on Power Systems*, vol. 22, pp. 1851–1860, Nov 2007.
- [4] A. Laifa and M. Boudour, "Facts allocation for power systems voltage stability enhancement using mopso," in *Systems, Signals and Devices, 2008. IEEE SSD 2008. 5th International Multi-Conference on*, pp. 1–6, IEEE, 2008.
- [5] W. Ongsakul and P. Jirapong, "Optimal allocation of facts devices to enhance total transfer capability using evolutionary programming," in *Circuits and Systems, 2005. ISCAS 2005. IEEE International Symposium on*, pp. 4175–4178, IEEE, 2005.
- [6] M. M. Farsangi, H. Nezamabadi-pour, Y.-H. Song, and K. Y. Lee, "Placement of svc's and selection of stabilizing signals in power systems," *IEEE Transactions on Power Systems*, vol. 22, no. 3, pp. 1061–1071, 2007.
- [7] S. Gerbex, R. Cherkaoui, and A. J. Germond, "Optimal location of multi-type facts devices in a power system by means of genetic algorithms," *IEEE transactions on power systems*, vol. 16, no. 3, pp. 537–544, 2001.
- [8] S. Sakthivel, D. Mary, R. Vetrivel, and V. S. Kannan, "Optimal location of svc for voltage stability enhancement under contingency condition through pso algorithm," *International Journal of Computer Applications (0975–8887)*, vol. 20, no. 1, 2011.
- [9] A. Kasis, E. Devane, C. Spanias, and I. Lestas, "Primary frequency regulation with load-side participation Part I: stability and optimality," *IEEE Transactions on Power Systems*, vol. 32, no. 5, pp. 3505–3518, 2017.
- [10] A. J. van der Schaft and B. M. Maschke, "Port-Hamiltonian systems on graphs," *SIAM Journal on Control and Optimization*, vol. 51, no. 2, pp. 906–937, 2013.
- [11] S. Fiaz, D. Zonetti, R. Ortega, J. Scherpen, and A. Van der Schaft, "A port-hamiltonian approach to power network modeling and analysis," *European Journal of Control*, vol. 19, no. 6, pp. 477–485, 2013.
- [12] C. Spanias and I. Lestas, "A system reference frame approach for stability analysis and control of power grids," under review, 2018.
- [13] J. Bao, P. L. Lee, and B. E. Ydstie, *Process control: the passive systems approach*. PhD thesis, Springer-Verlag, 2007.
- [14] C. Taylor, G. Scott, and A. Hammad, "Static var compensator models for power flow and dynamic performance simulation," *IEEE Transactions on Power Systems (Institute of Electrical and Electronics Engineers) (United States)*, vol. 9:1, Feb 1994.
- [15] J. Chow, G. Rogers, and K. Cheung, "Power system toolbox," *Cherry Tree Scientific Software*, [Online] Available: <http://www.ecse.rpi.edu/pst/PST.html>, vol. 48, p. 53, 2000.
- [16] P. Kundur, N. J. Balu, and M. G. Lauby, *Power system stability and control*, vol. 7. McGraw-hill New York, 1994.
- [17] H. K. Khalil, *Nonlinear Systems*. New Jersey: Prentice Hall, 2002.
- [18] R. Bhatia, *Positive definite matrices*. Princeton university press, 2009.
- [19] R. A. Horn and C. R. Johnson, *Matrix analysis*. Cambridge university press, 2012.
- [20] N. Kottenstette and P. J. Antsaklis, "Relationships between positive real, passive dissipative, & positive systems," in *Proceedings of the 2010 American control conference*, pp. 409–416, IEEE, 2010.
- [21] E. Devane, A. Kasis, C. Spanias, M. Antoniou, and I. Lestas, "Distributed frequency control and demand-side management," in *Smarter Energy: From Smart Metering to the Smart Grid* (H. Sun, N. Hatziar-gyriou, L. Carpanini, H. V. Poor, and M. A. S. Forni , eds.), ch. 9, pp. 157–192, IET, 2016.
- [22] E. Devane, A. Kasis, M. Antoniou, and I. Lestas, "Primary frequency regulation with load-side participation Part II: beyond passivity approaches," *IEEE Transactions on Power Systems*, vol. 32, no. 5, pp. 3519–3528, 2017.
- [23] M. J. McCourt and P. J. Antsaklis, "Demonstrating passivity and dissipativity using computational methods," *ISIS*, p. 008, 2013.
- [24] G. Rogers, *Power system oscillations*. Springer Science & Business Media, 2012.
- [25] J. Machowski, J. Bialek, and J. Bumby, *Power system dynamics: stability and control*. John Wiley & Sons, 2011.